Ranking of parameters in bioheat transfer using Taguchi analysis

Jamil, Muhammad; Ng, Eddie Yin-Kwee

2013

Jamil, M., & Ng, E. Y. K. (2012). Ranking of parameters in bioheat transfer using Taguchi analysis. International Journal of Thermal Sciences, 63, 15-21.

https://hdl.handle.net/10356/95315

https://doi.org/10.1016/j.ijthermalsci.2012.07.002

Ranking of parameters in bioheat transfer using Taguchi analysis

Muhammad Jamil, E.Y.K. Ng*

School of Mechanical and Aerospace Engineering, College of Engineering, Nanyang Technological University, 50 Nanyang Avenue, 639798 Singapore, Singapore

** Corresponding author.*

E-mail address: mykng@ntu.edu.sg (E.Y.K. Ng).

Abstract

Modeling bioheat transfer plays an important role in the treatment planning of cancer therapy. Historically, Pennes bioheat equation has been used for bioheat transfer modeling in living tissue because of its simplicity, effectiveness and ease of application. It is imperative that the effect of each parameter involved in the bioheat transfer be known. The ultimate goal of a cancer treatment is to maximize the damage to the cancer affected tissue and minimize the collateral damage to the normal tissue surrounding it. This study takes into account six 3-level factors namely blood perfusion rate in healthy tissue and tumor, frequency, applied voltage, metabolic heating rate in healthy tissue and tumor. The purpose of this study is to rank the parameters involved in electromagnetic heating and determine the factors which affect the bioheat transfer the most. Maximum obtained temperature was taken as the response variable and Taguchi orthogonal arrays were used to obtain required data with minimum number of numerical experiments required. Calculations were performed in Minitab statistical software. The results show that the applied voltage has the largest effect on the maximum achieved temperature followed by frequency of the electromagnetic radiation.

Keywords:
Bioheat transfer
Quasi-static approximation
Electromagnetic heating
Hyperthermia system
Cancer treatment planning
Taguchi orthogonal arrays

1. Introduction

Hyperthermia is a condition in which the heat generated in the body cannot be dissipated by the natural thermoregulatory mechanisms. Hyperthermia can be induced naturally or artificially. Fever is the natural form of hyperthermia in which body's defense mechanism is activated and body raises its temperature to counteract the invaders in the form of germs. Hyperthermia therapy is a therapy used in cancer treatment. It involves raising the temperature of the cancer affected area above 42 $^{\circ}$C. At this temperature, heat cannot be dissipated effectively through natural mechanisms and results in permanent thermal damage to biological material. The heating effect is obtained using external electromagnetic field. A predefined voltage is applied across the electrodes and desired heating effect is obtained with induction heating in the tissue. From a medical practitioner's point of view, effect of each parameter during the treatment is crucial and can affect the outcome of the treatment. So it is imperative to quantify the effect of each independent parameter used in the treatment exercise.

Previous studies on the bioheat transfer have suggested that temperature plays an important role in the treatment in the hyperthermia therapy [1−3] and very high temperature can result in sudden death of the cell [1,4,5]. Based on the previous studies it is a well known fact now that maximum achieved temperature plays vital part in outcome of the treatment. Various studies quantifying the lethal effects of temperature on the tissues have been carried out and many thermal models have been proposed [6−9].

The basic purpose of the hyperthermia treatment is to raise the tumor temperature above tolerable limits without causing thermal damage to the surrounding healthy tissue. A slight discrepancy in temperature control mechanism could result in irreversible thermal damage to the patient which in worst case scenario can also cause death.

The motivation behind this research is to rank the parameters which affect the temperature inside the biological tissue. For electromagnetic heating, the maximum achieved temperature depends on the electric field strength inside the biological material. The electric field generated inside the biological material can be calculated using Maxwell's equations. Furthermore, if the wavelength of the radiation is much larger than the size of the object, quasi-static approximation can be used. The electric field strength inside the tissue in a Cartesian domain X, can be obtained by evaluating the scalar potential inside the tissue [10,11] i.e.,

$$\nabla \cdot [\varepsilon(X) \cdot \nabla \varphi(X)] = 0 \tag{1}$$

where ε represents permittivity of the material.

Electric field strength E can be evaluated by finding the negative gradient of scalar potential in the tissue.

$$E(X) = -\nabla \varphi(X) \tag{2}$$

The electric energy induced in the tissue dissipates in the form of heat. The volumetric generation of heat due to electric field inside the tissue is given by:

$$Q_r(X,t) = \frac{\sigma |E(X)|^2}{2} = \frac{\sigma \left[|E_x|^2 + |E_y|^2 + |E_z|^2 \right]}{2} \tag{3}$$

where σ represents the electrical conductivity of the tissue.

It can be seen that the volumetric heat generated in the tissue due to electric field depends on the electrical conductivity σ and electric field strength inside the tissue.

Electromagnetic heating in the tissue represents an electrothermal problem. For calculation of temperature field in the tissue many thermal models have been proposed [12−14] but Pennes bioheat model [15] is the most popular one because of its simplicity, ease of application and effectiveness in most cases. Pennes model has been used by many researchers for the heat transfer in biological materials [3,10,11,13,16−19].

The heat transfer inside the tissue can be represented by Pennes equation:

$$\rho c \frac{\partial T(X,t)}{\partial t} = \nabla \cdot [k(X) \nabla T(X,t)] + G_{be} c_b [T_a - T(X,t)] + Q(X,t) \quad X \in \Omega \tag{4}$$

The temperature of the body is maintained by the metabolic heat generated in the body. The effect of metabolic heat also needs to be considered. In Pennes equation, this effect is accommodated in $Q(X,t)$ which includes the heat generated by external electromagnetic field $Q_r(X,t)$ and metabolic heat $Q_{met}(X,t)$ generated by natural mechanisms of the body. The solution of the system of equations resulting from the application of Pennes bioheat equation in tissue and tumor would result in accurate information about the temperature inside the biological material.

For biological tissues metabolic heat is vital for survival. The energy required for replenishment is generated by the oxidation of the nutrients supplied to the biological tissues. Any decrease in metabolic heat would mean an increase in the input energy to attain hyperthermia and vice versa. Blood perfusion is also an important parameter which is responsible for transfer of energy via convection. During the electrode based thermal therapy if blood perfusion is increased, it could flush away the supplied energy. Furthermore, the blood escaping out of the treatment zone could cause collateral damage to the peripheral normal tissue and would make it difficult to

achieve hyperthermic conditions.

Frequency and applied voltage are also critical to the electrode based thermal therapy. Frequency and voltage affect the electromagnetic energy being delivered to the treatment zone. A higher voltage would mean an increased energy input and changes in frequency would result in changes in electrical conductivity and permittivity of the biological material which in turn also affects the heat being delivered as can be seen from Eq. (3). For hyperthermia treatment different frequencies can be utilized depending on the nature of the problem. The nature of interaction with the material is dependent on the frequency being used. It has been noted that penetration depth and the amount of energy delivered are strong functions of frequency [17,20−22]. Varying frequency results in a corresponding change in the electrical conductivity and dielectric properties of the material.

Table 1 lists the electromagnetic properties of the tissue at different frequencies.

2. Taguchi design of experiments

For the ranking of parameters, six parameters were considered as shown in Table 2.

For each of the six parameters, 3 levels namely low, medium and high were considered. These six factors having 3 different levels constitute the array with minimum number of experimental combinations (MNE) given by k^n, where $k =$ number of levels, $n =$ number of factors considered.

For current analysis, for 6 parameters having 3 levels it gives $3^6 = 729$ experimental combinations. A full factorial design utilizing all the combinations would become very tedious and would add to the complexity of the problem. To overcome this problem, Taguchi's orthogonal array can be utilized to give the similar results but with much less number of experiments required.

For Taguchi analysis standard L-27 orthogonal array was thus used which gives minimum number of experiments needed for the parameters outlined above with corresponding levels.

3. Development of numerical model for hyperthermia therapy

In order to evaluate the correct nature of interaction between the parameters, the FEM numerical methodology needs to be tested. Only then the definite nature of the interaction between the parameters can be found out. For this purpose, 3D problem used in the study by Deng et al. [11] was first benchmarked in which Monte Carlo algorithm was used. The geometry of the problem used is shown in Fig. 1.

The numerical domain consists of 0.08 m × 0.8 m × 0.08 m and the heating area is given as:

$$\Omega' \subseteq [x = 0.0, 0.03\ \text{m} \le y \le 0.05\ \text{m},\ 0.03 \le z \le 0.05\ \text{m}] \cup [x = 0.016\ \text{m},\ 0.03\ \text{m} \le y \le 0.05\ \text{m},\ 0.03 \le z \le 0.05\ \text{m}]$$

The tumor domain is given by:

$$\Omega_2 \subseteq [0.02\ \text{m} \le x \le 0.04\ \text{m},\ 0.03 \le y \le 0.05\ \text{m},\ 0.03 \le z \le 0.05\ \text{m}]$$

For steady state the heat transfer inside the tissue can be represented by Pennes equation:

$$\nabla \cdot [k_e(X) \nabla T_e(X)] + \rho_b \omega_{be} c_b [T_a - T_e(X)] + Q_e(X) = 0 \quad X \in \Omega_e \tag{5}$$

Subscript e = 1, refers to normal tissue and e = 2 refers to tumor.

In order to prevent overheating of the surface, cooling pads are often used in electrode based thermal therapy as shown in Fig. 1. This can be represented by

convection boundary condition on the surface. Also at the middle of the domain, body core temperature is assumed. Thermal insulation is assumed at all other boundaries. For the current research same value of thermal conductivity was used for tissue and tumor as was done by Deng et al [11].

The boundary conditions are:

$$\begin{cases} -k_1\dfrac{\partial T_1}{\partial x} = 0 & x = 0, L \\ -k_1\dfrac{\partial T_1}{\partial y} = 0 & y = 0, L \\ -k_1\dfrac{\partial T_1}{\partial z} = h_w(T_1 - T_w) & z = 0 \\ T_1 = T_o & z = L \end{cases} \tag{6}$$

where h_w is the convection coefficient of the cooling water and T_w is the temperature of the cooling water. T_0 represents body core temperature.

For the 3D analysis following thermal properties were used.

$\rho_b = 1000\ \text{kg/m}^3,\ c_b = 4200\ \text{J/kg.K},$
$T_a = 37\ ^\circ\text{C},\ k = 0.5\ \text{W/m.}^\circ\text{C},\ L = 0.08\ \text{m},$
$h_w = 100\ \text{W/m}^2.^\circ\text{C}, T_w = 10\ ^\circ\text{C}.$

As can be seen from Fig. 2, the results obtained using FEM and Monte Carlo method are very similar and have same profiles of heat source and temperature for the same treatment conditions. It can also be deduced that the results obtained by FEM are reliable and such bioheat applications involving electromagnetic heating can be successfully simulated using FEM.

As a number of experiments need to be undertaken for this study, which would take longer time to complete, a 2-D analysis is sufficient for this study keeping in view the scope of this study. A 2-D study allows quick acquisition of data needed to perform the Taguchi analysis with milder restrictions on computational resources and memory requirements. As the tumor in reality is three dimensional in nature, it still needs to be tested whether the 2-D simulation using FEM is sufficient or not. In order to use 2-D configuration, first the results need to be validated against some previous study. For

two-dimensional analysis model used by Ewa et al. [10] was utilized as a benchmark for the current study. Ewa used boundary element method (BEM) to simulate the problem as shown in Fig. 3.

At the interface of healthy tissue and tumor continuity of electric flux and electric potential was assumed. A specified potential U was applied across the electrodes as shown in Fig. 3 while all other boundaries were assumed to be insulated. The computational domain shown in Fig. 4 is subject to following boundary conditions.

At the interface of skin and tumor, continuity of electric flux and potential is assumed.

$$(x,y)\in \Gamma_c : \begin{cases} \varphi_1(x,y) = \varphi_2(x,y) \\ -\varepsilon_1 \dfrac{\partial \varphi_1(x,y)}{\partial n} = -\varepsilon_2 \dfrac{\partial \varphi_2(x,y)}{\partial n} \end{cases} \tag{7}$$

Electrical potential U is applied across the electrode surfaces.

$$\begin{aligned} (x,y)\in \Gamma_1 : &\quad \varphi_1(x,y) = U \\ (x,y)\in \Gamma_2 : &\quad \varphi_2(x,y) = -U \end{aligned} \tag{8}$$

Electrical insulation is assumed on all other boundaries.

$$(x,y)\in \Gamma_3 \cup \Gamma_4 \cup \Gamma_5 \cup \Gamma_6 \cup \Gamma_7 \cup \Gamma_8 : -\varepsilon_1 \frac{\partial \varphi_1(x,y)}{\partial n} = 0 \tag{9}$$

The bioheat transfer in the specified domain can be described by the Pennes bioheat equation [15]:

$$(x,y)\in \Omega_e : k_e \nabla^2 T_e(x,y) + \rho_b \omega_{be} c_b [T_a - T_e(x,y)] + Q_e(x,y) = 0 \tag{10}$$

And assuming continuity of temperature and heat flux across the interface between healthy tissue and tumor, the boundary conditions are:

$$(x,y)\in\Gamma_c:\begin{cases} T_1(x,y) = T_2(x,y) \\ -k_1\dfrac{\partial T_1(x,y)}{\partial n} = -k_2\dfrac{\partial T_2(x,y)}{\partial n} \end{cases} \tag{11}$$

Negative sign above shows that the heat flow is towards the negative temperature gradient. At all the other boundaries, convection boundary condition was assumed:

$$(x,y)\in\Gamma_1\cup\Gamma_2\cup\Gamma_3\cup\Gamma_4\cup\Gamma_5\cup\Gamma_6 : -k_1\frac{\partial T_1(x,y)}{\partial n} = h_w[T_1(x,y) - T_w] \tag{12}$$

Frequency has significant effect on the electromagnetic properties of the material. Depending on the frequency being used, EM properties change significantly. Electromagnetic properties used for healthy tissue and tumor are shown in Table 3 below.

In order to get reliable results, a mesh independence study was carried out first. The grid consisted of triangular elements and grid size was progressively refined from coarse to fine. Finally grid consisting of 35,680 elements was selected for the current analysis. The calculation domain is 0.08 m × 0.04 m. The tumor region spans Ω_2 = [0.032 m ≤x ≤ 0.048 m, 0.016 ≤ y ≤ 0.032 m] and heating area is described as: Ω' = [{0.032 m ≤x ≤ 0.048 m, y = 0}, {0.032 m ≤x ≤ 0.048 m, y = 0.04 m}].

Fig. 5 compares the temperature profile obtained from BEM and FEM. It can be seen that both methods give similar results.

4. Numerical simulation and data acquisition for matrix experiment

After developing the numerical configuration, Taguchi design of experiment analysis was carried out using Minitab Software. For six parameters having three levels each, standard L-27 orthogonal array was used. For the current analysis, maximum temperature in the domain was chosen as the response variable. Table 4 shows the maximum temperature under the influence of varying parameters.

5. Results and discussion

After obtaining the data matrix for L-27 array, Analysis of Variance (ANOVA) was carried out on the data predicted. The main purpose of carrying out ANOVA is to quantify the effect of each of the parameters on the response variable. Details of ANOVA can be found in Refs. [27−29]. Results of ANOVA are included in Table 5.

Table 5 reveals that applied voltage (*V*) and frequency (*f*) constitute the major effect on the maximum temperature achieved. Both the parameters account for about 90% of the effect in the response i.e., maximum achievable temperature. Tissue metabolic rate (Q_{met1}) is the third major contributing factor in the response. Furthermore, the interaction between the variables is insignificant.

Fig. 6 shows the main effects plot for temperature of the six variables selected for Taguchi analysis.

Fig. 6 suggests that applied voltage (*V*) and frequency (*f*) followed by tissue metabolic rate (Q_{met1}) are the major variables affecting the response. It can also be observed that a linear increase in the input parameters like frequency or voltage doesn't result in corresponding linear increase in temperature. For example, effect of increasing voltage or frequency from low to medium is not the same as raising them from medium to high although the change interval are same as can be seen in Table 3 from low to medium and from medium to high. This effect can be clearly seen in Fig. 6 by response having different slopes in each interval.

It can also be concluded that for the six variables used in analysis each having three levels as shown in Table 2, the best arrangement would be to keep Q_{met2}, f and V at high levels and Q_{met1}, ω_{b1} and ω_{b2} at low levels. This also suggests that lower blood perfusion rate would favor a higher achievable temperature. This result can be very important for treatment planning. Tumor is a complex and irregular structure formed by the uncontrolled growth of cells having characteristic behavior. Most often there is

a large vein which supplies blood to the tumor. If before the treatment, that vein is plugged which would cause a reduced supply of blood to the tumor, higher temperature can be achieved with the same treatment arrangement.

6. Conclusions

Taguchi's design of experiments was used in an attempt to rank the parameters in hyperthermia therapy treatment planning which is based on Pennes bioheat equation. Six parameters namely tumor metabolic rate, tissue metabolic rate, tissue blood perfusion, tumor blood perfusion, voltage and frequency were considered and it was concluded that voltage and frequency are the most important factors to consider during the hyperthermia treatment planning. It is also important for a medical practitioner to know that blood perfusion in tissue and tumor can also have significant effect on the maximum achieved temperature. As per the literature on characteristic of the tumor, in some cases tumor gets its supply of oxygen and nutrients from a single large vein. If this blood supply is reduced partially or completely by plugging the vein, it shall greatly improve the efficacy of the treatment. From medical practitioner's point of view, the information regarding the parameters involved in the therapy is of utmost importance and any irregularity, out of lack of knowledge or negligence on the part of the practitioner, could result in lethal outcome. This study concludes that applied voltage and frequency are the most important parameters that could affect the outcome of the therapy. The practitioner must prioritize the parameters involved and careful consideration must be made for the selection of most important parameters involved i.e. voltage and frequency.

References

[1] A. Ito, H. Honda, T. Kobayashi, Cancer immunotherapy based on intracellular hyperthermia using magnetite nanoparticles: a novel concept of "heat-controlled necrosis" with heat shock protein expression, Cancer Immunology, Immunotherapy 55 (2006) 320−328.

[2] A. Ito, M. Shinkai, H. Honda, K. Yoshikawa, S. Saga, T. Wakabayashi, J. Yoshida, T. Kobayashi, Heat shock protein 70 expression induces antitumor immunity during intracellular hyperthermia using magnetite nanoparticles, Cancer Immunology, Immunotherapy 52 (2003) 80−88.

[3] S.B. Field, C.C. Morris, The relationship between heating time and temperature: its relevance to clinical hyperthermia, Radiotherapy and Oncology 1 (1983) 179−186.

[4] G. Nedelcu, Magnetic nanoparticles impact on tumoral cells in the treatment by magnetic fluid hyperthermia, Digest Journal of Nanomaterials and Biostructures 3 (2008) 103−107.

[5] S.V. Gomonov, V.M. Efanov, Theoretical model of irreversible intracellular electroporation (supra-electroporation) in a single cell, in: IEEE International Power Modulators and High Voltage Conference, Proceedings of the 2008, 2008, pp. 330−333.

[6] F.C. Henriques, A.R. Moritz, Studies of thermal injury. I. The conduction of heat to and through skin and the temperatures attained therein − a theoretical and experimental investigation, American Journal of Pathology 23 (1947) 531.

[7] Y.S. Xu, R.Z. Qian, Analysis of thermal injury process based on enzyme deactivation mechanisms, Journal of Biomechanical Engineering-Transactions of the ASME 117 (1995) 462−465.

[8] A.S. Stephen, C.D. William, Thermal dose determination in cancer therapy, International Journal of Radiation Oncology, Biology, Physics 10 (1984) 787−800.

[9] W.C. Dewey, L.E. Hopwood, S.A. Sapareto, L.E. Gerweck, Cellular responses to combinations of hyperthermia and radiation, Radiology 123 (1977) 463−474.

[10] E. Majchrzak, G. Dziatkiewicz, M. Paruch, The modelling of heating a tissue subjected to external electromagnetic field, Acta of Bioengineering and Biomechanics 10 (2008) 29−37.

[11] Y.G. Lv, Z.S. Deng, J. Liu, 3-D numerical study on the induced heating effects of embedded micro/nanoparticles on human body subject to external medical electromagnetic field, IEEE Transactions on NanoBioscience 4 (2005) 284−294.

[12] F.M. Waterman, L. Tupchong, R.E. Nerlinger, J. Matthews, Blood flow in human tumors during local hyperthermia, International Journal of Radiation Oncology, Biology, Physics 20 (1991) 1255−1262.

[13] F. Xu, T. Lu, Skin bioheat transfer and skin thermal damage, in: Introduction to Skin Biothermomechanics and Thermal Pain, Springer Berlin Heidelberg, 2011, pp. 23−68.

[14] E.Y.K. Ng, H.M. Tan, E.H. Ooi, Boundary element method with bioheat equation for skin burn injury, Burns 35 (2009) 987−997.

[15] H.H. Pennes, Analysis of tissue and arterial blood temperature in the resting human forearm, Journal of Applied Physiology 1 (1948) 93−122.

[16] Y. Rabin, Is intracellular hyperthermia superior to extracellular hyperthermia in the thermal sense? International Journal of Hyperthermia 18 (2002) 194−202.

[17] R.E. Rosensweig, Heating magnetic fluid with alternating magnetic field, Journal of Magnetism and Magnetic Materials 252 (2002) 370−374.

[18] Z.-S. Deng, J. Liu, Theoretical evaluation on the thermal effects of extracellular hyperthermia and intracellular hyperthermia, ASME Conference Proceedings 2007 (2007) 827−828.

[19] T.C. Shih, P. Yuan, W.L. Lin, H.S. Kou, Analytical analysis of the Pennes bioheat transfer equation with sinusoidal heat flux condition on skin surface, Medical Engineering & Physics 29 (2007) 946−953.

[20] M.A. Stuchly, T.W. Athey, S.S. Stuchly, G.M. Samaras, G. Taylor, Dielectric properties of animal tissues in vivo at frequencies 10 MHze1 GHz, Bio-electromagnetics 2 (1981) 93−103.

[21] S.A. Curley, Radio frequency ablation of malignant liver tumors, Oncologist 6 (2001) 14−23.

[22] A.S. Eggeman, S.A. Majetich, D. Farrell, Q.A. Pankhurst, Size and concentration effects on high frequency hysteresis of iron oxide nanoparticles, IEEE Transactions on Magnetics 43 (2007) 2451−2453.

[23] F.S. Barnes, C.L.J. Hu, Model for some nonthermal effects of radio and microwave fields on biological membranes, IEEE Transactions on Microwave Theory and Techniques 25 (1977) 742−746.

[24] M.M. Osman, E.M. Afify, Thermal modeling of the malignant woman's breast, Journal of Biomechanical Engineering 110 (1986) 269−276.

[25] J. Werner, M. Buse, Temperature profiles with respect to inhomogeneity and geometry of the human body, Journal of Applied Physiology 65 (1988) 1110−1118.

[26] Z.S. Deng, J. Liu, Monte Carlo method to solve multidimensional bioheat transfer problem, Numerical Heat Transfer, Part B: Fundamentals 42 (2002) 543−567.

[27] J. Antony, Design of Experiments for Engineers and Scientists, Butterworth-Heinemann, 2003.

[28] E.Y.K. Ng, W.K. Ng, J. Huang, Y.K. Tan, The engineering analysis of bioheat equation and penile hemodynamic relationships in the diagnosis of erectile dysfunction: part II − model optimization using the ANOVA and Taguchi method, International Journal of Impotence Research 20 (2008) 285−294.

[29] N.M. Sudharsan, E.Y.K. Ng, Parametric optimization for tumour identification bioheat equation using ANOVA and the Taguchi method, Proceedings of the Institution of Mechanical Engineers, Part H: Journal of Engineering in Medicine 214 (2000) 505−512.

Glossary

c: specific heat [J/(kg K)]
c_b: specific heat of blood [J/(kg K)]
E: electric field intensity (V/m)
F: Fisher statistic
f: frequency (Hz)
G_b: blood perfusion rate (1/s)
h_w: convection coefficient between skin and water [W/(m^2 K)]
k: thermal conductivity [W/(m K)]
k: number of levels
L: length of the side of numerical domain (m)
n: number of parameters
P: probability value
Q: volumetric heat generation rate (W/m^3)
Q_{met}: metabolic heat generation rate (W/m^3)
Q_r: spatial heat source (W/m^3)
T: temperature (K)
T_0: body core temperature (K)
T_a: arterial blood temperature (K)
T_w: temperature of the cooling water (K)
U: electrode potential (V)

Greek symbols
ε: permittivity of the material (F/m)
ε_0: permittivity of the free space (F/m)
ε_r: relative permittivity of the material
ρ: density (kg/m^3)
ρ_b: density of blood (kg/m^3)
σ: electrical conductivity of the material (Ω^{-1} m^{-1})
φ: electric scalar potential (V)
Ω: numerical domain
Ω': domain of the heating electrode

Subscripts
1: normal tissue domain
2: tumor domain
a: artery
b: blood
e: domain number
met: metabolic heat
w: water

Abbreviations
ANOVA: Analysis of Variance
DF: degrees of freedom
MNE: minimum number of experimental combinations
SS: sum of squares adj
MS: adjusted mean sum of squares

List of Tables

Table 1 Frequency-dependent electromagnetic characteristics of skin tissue [23].

Table 2 Parameters with corresponding levels used for analysis.

Table 3 Electromagnetic properties used for tissue and tumor domain [10].

Table 4 Taghuchi L-27 array with corresponding response values of maximum temperature in the domain.

Table 5 ANOVA table for the selected parameters and interactions.

List of Figures

Fig. 1 3D hyperthermia system with cooling pads [11].

Fig. 2 3D comparison of steady state heat source (a) and temperature (b) at section z = 0.04 m at f = 1 MHz, U = 10 V.

Fig. 3 Two-dimensional hyperthermia system used for analysis [10].

Fig. 4 Numerical domain with boundary conditions [10].

Fig. 5 Temperature distribution at f = 1 MHz and U = 10 V.

Fig. 6 Main effects plot for temperature.

Frequency f [MHz]	Electrical gr3 conductivity σ_1 [S/m]	Dielectric constant ε_1 [C^2/N m^2]
0.001	0.102	$100{,}000\varepsilon_0$
0.01	0.114	$50{,}000\varepsilon_0$
0.1	0.192	$20{,}000\varepsilon_0$
1	0.40	$2000\varepsilon_0$
10	0.625	$100\varepsilon_0$

The dielectric constant of the vacuum ε_0 is 0.8538×10^{-12} C^2/N m^2.

Table 1

Table 2

Factor	Units	Level 1 (low)	Level 2 (medium)	Level 3 (high)
Tissue metabolic rate (Q_{met1})	(W/m^3)	800 [15]	1200 [15]	4200 [11]
Tumor metabolic heat source (Q_{met2})	(W/m^3)	700 [24]	42,000 [11]	65,400 [24]
Tissue blood perfusion rate (ω_{b1})	(1/s)	0.0002 [25]	0.00035 [25]	0.00057 [25]
Tumor blood perfusion rate (ω_{b2})	(1/s)	0.002 [26]	0.007 [25]	0.015 [25]
Frequency (f)	(MHz)	0.1 [10]	1 [10]	10 [10]
Voltage (V)	(V)	5 [11]	10 [11]	15 [11]

S. no	Frequency f [MHz]	Dielectric permittivity [$C^2/N\ m^2$]		Electrical conductivity [S/m]	
		ε_1	ε_2	σ_1	σ_2
1	0.1	$20{,}000\varepsilon_0$	$1.2\varepsilon_1$	0.192	$1.2\sigma_1$
2	1	$2000\varepsilon_0$	$1.2\varepsilon_1$	0.4	$1.2\sigma_1$
3	10	$100\varepsilon_0$	$1.2\varepsilon_1$	0.625	$1.2\sigma_1$

Table 3

Experiment no.	f	V	Q_{met1}	ω_{b1}	Q_{met2}	ω_{b2}	Max. temperature
1	0.1	5	800	0.0002	700	0.002	33.307
2	1	10	800	0.0002	700	0.002	40.71
3	10	15	800	0.0002	700	0.002	70.4
4	0.1	5	800	0.00035	42,000	0.007	37.229
5	1	10	800	0.00035	42,000	0.007	40.484
6	10	15	800	0.00035	42,000	0.007	63.305
7	0.1	5	800	0.00057	65,400	0.015	37.733
8	1	10	800	0.00057	65,400	0.015	39.993
9	10	15	800	0.00057	65,400	0.015	59.336
10	0.1	10	1200	0.00035	700	0.015	37.069
11	1	15	1200	0.00035	700	0.015	50.092
12	10	5	1200	0.00035	700	0.015	36.978
13	0.1	10	1200	0.00057	42,000	0.002	39.45
14	1	15	1200	0.00057	42,000	0.002	52.749
15	10	5	1200	0.00057	42,000	0.002	38.929
16	0.1	10	1200	0.0002	65,400	0.007	38.683
17	1	15	1200	0.0002	65,400	0.007	52.923
18	10	5	1200	0.0002	65,400	0.007	38.447
19	0.1	15	4200	0.00057	700	0.007	41.034
20	1	5	4200	0.00057	700	0.007	36.725
21	10	10	4200	0.00057	700	0.007	44.775
22	0.1	15	4200	0.0002	42,000	0.015	41.12
23	1	5	4200	0.0002	42,000	0.015	37.462
24	10	10	4200	0.0002	42,000	0.015	45.388
25	0.1	15	4200	0.00035	65,400	0.002	45.074
26	1	5	4200	0.00035	65,400	0.002	39.585
27	10	10	4200	0.00035	65,400	0.002	49.173

Table 4

Factors	DF	SS	Adj MS	F	P	% Contribution	Ranking
Q_{met1}	2	117.95	58.973	1.52	0.292	6.376	3
Q_{met2}	2	5.4	2.699	0.07	0.934	0.294	5
ω_{b1}	2	4.75	2.373	0.06	0.941	0.252	6
ω_{b2}	2	33.55	16.774	0.43	0.668	1.804	4
f	2	517.07	258.536	6.66	0.03	27.936	2
V	2	1152.12	576.061	14.85	0.005	62.290	1
$Q_{met1} \times f$	4	21.5	5.375	0.14	0.962	0.587	
$Q_{met1} \times V$	4	17.22	4.305	0.11	0.974	0.461	
Residual error	6	232.83	38.805				
Total	26	2102.38					

Table 5

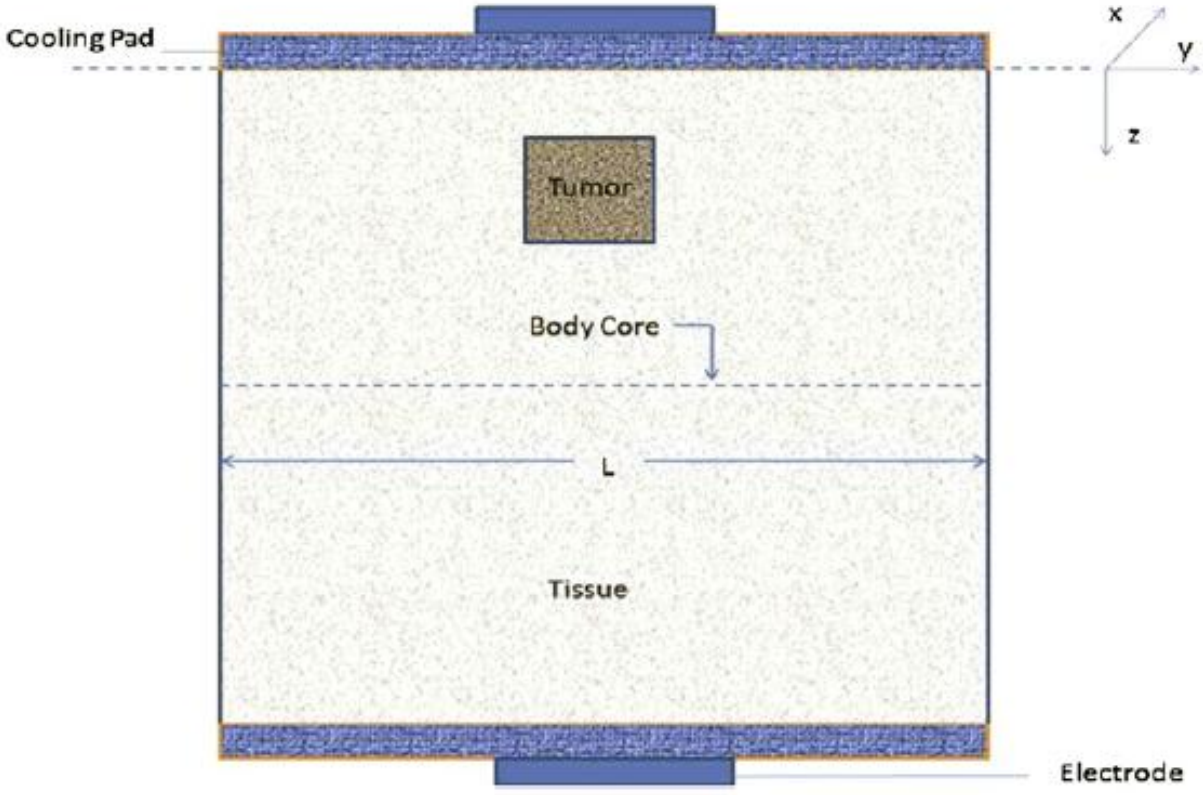

Fig. 1

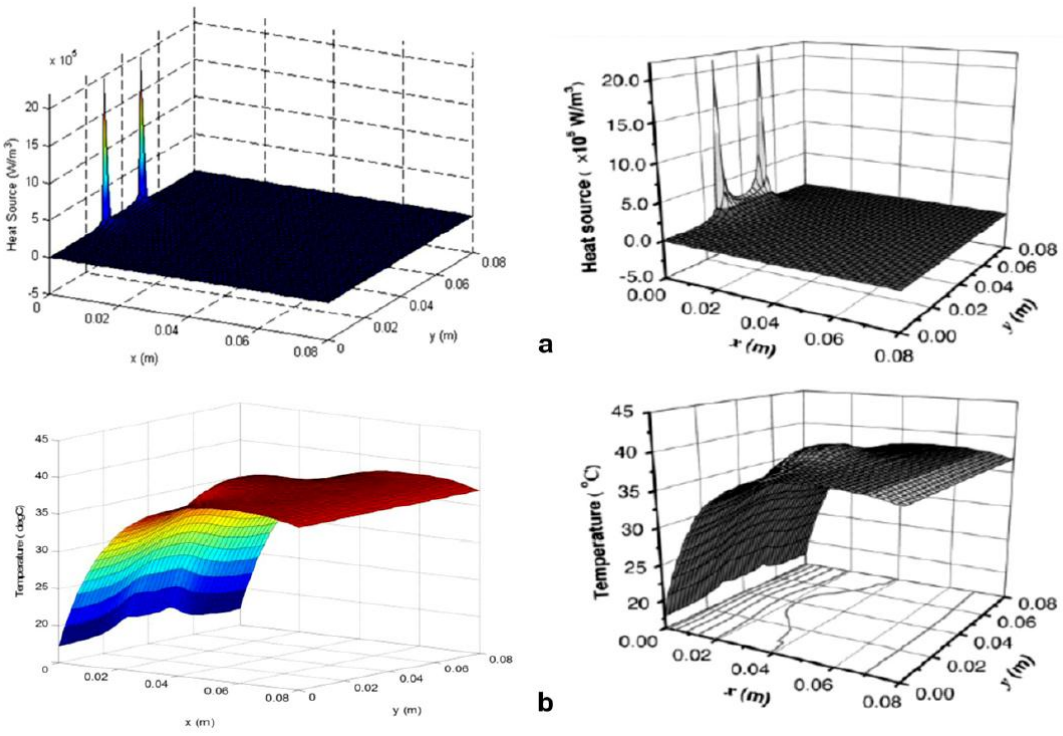
x 10^5
Heat Source (W/m^3)
x (m)
y (m)
a
Heat source (x10^5 W/m^3)
x (m)
y (m)
Temperature (deg C)
x (m)
y (m)
b
Temperature (°C)
x (m)
y (m)

Fig. 2

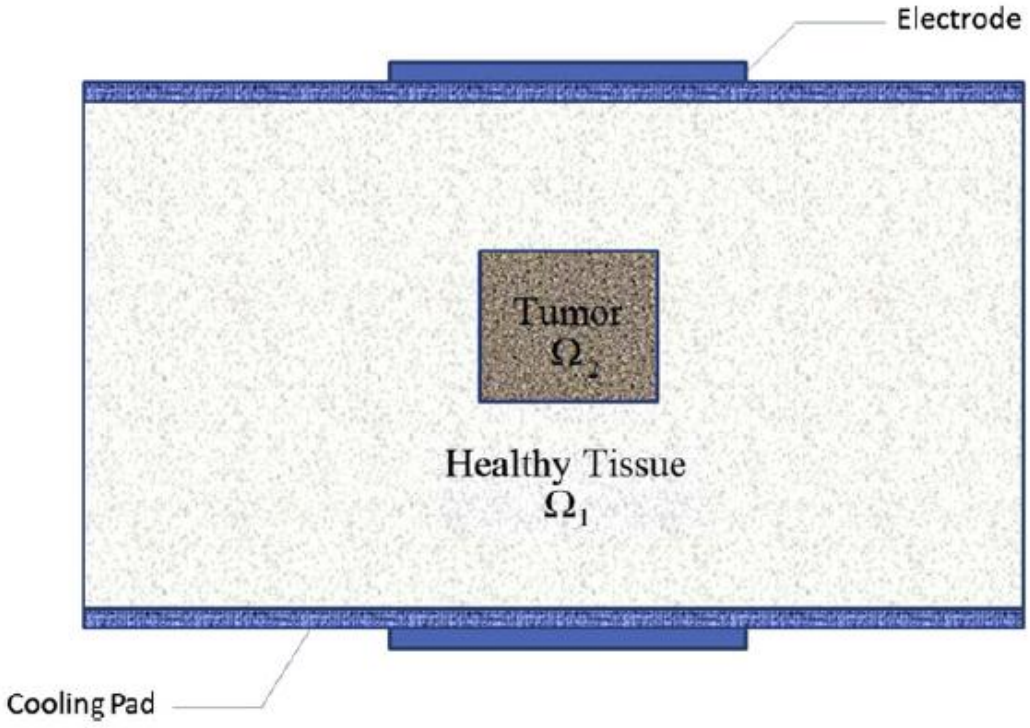

Fig. 3

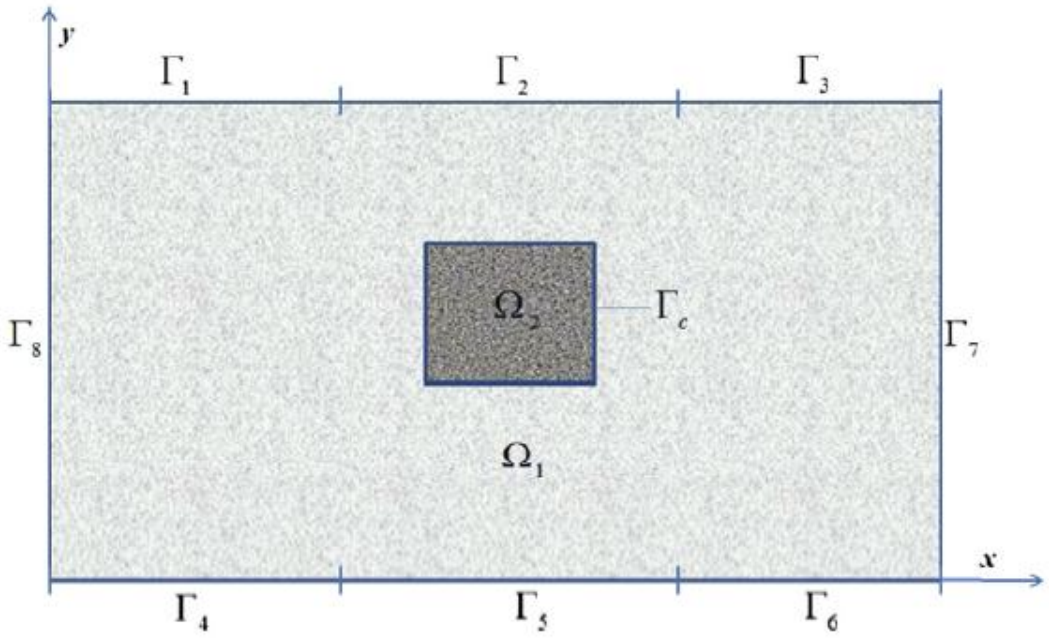

Fig. 4

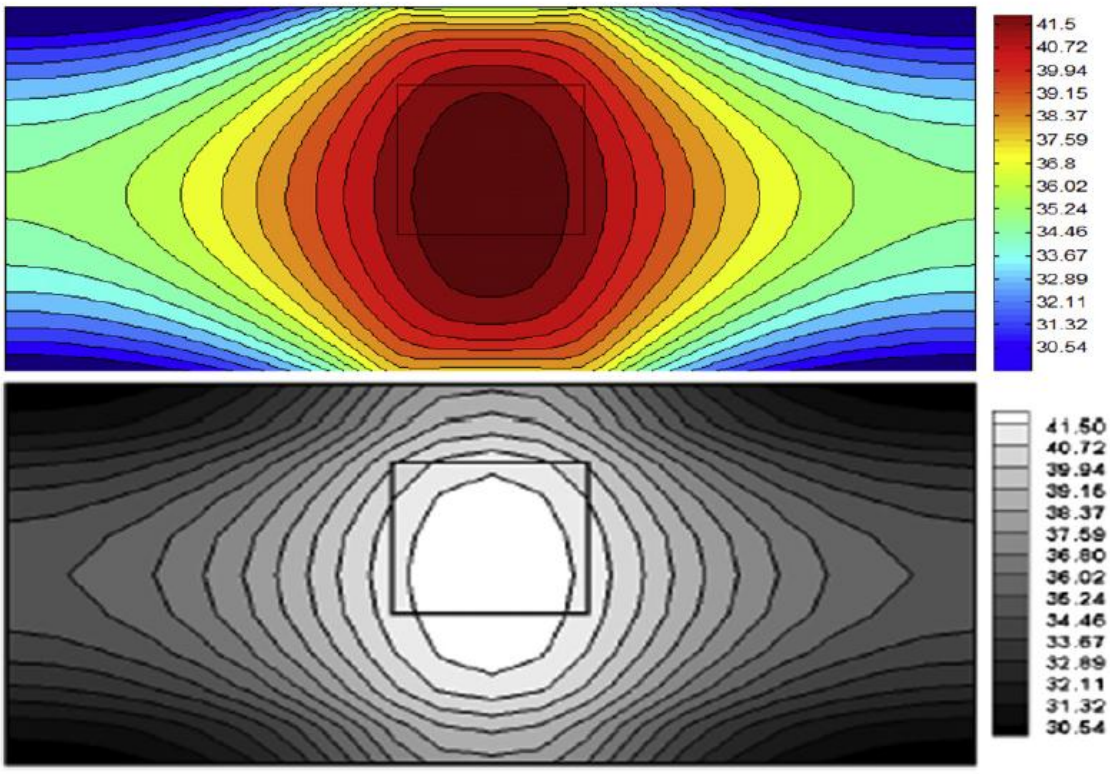
41.5
40.72
39.94
39.15
38.37
37.59
36.8
36.02
35.24
34.46
33.67
32.89
32.11
31.32
30.54
41.50
40.72
39.94
39.16
38.37
37.59
36.80
36.02
35.24
34.46
33.67
32.89
32.11
31.32
30.54

Fig. 5

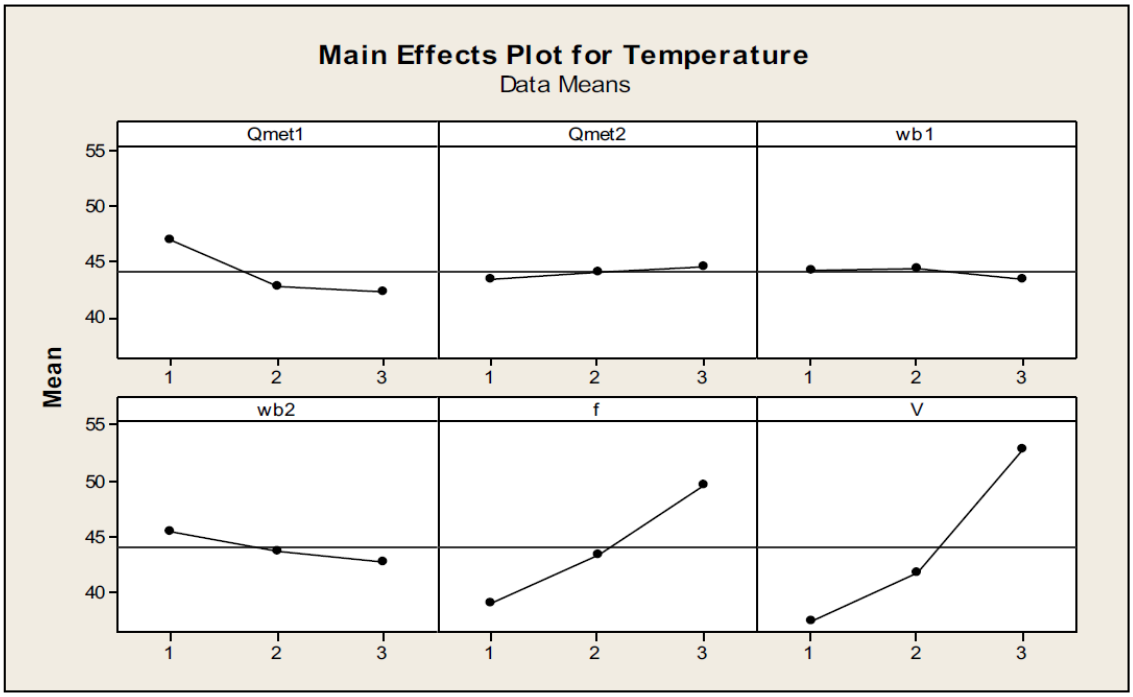
Main Effects Plot for Temperature
Data Means
Qmet1
Qmet2
wb1
wb2
f
V
Mean
55
50
45
40
1
2
3

Fig. 6